BIOLOGICAL SCIENCES

Biological sciences at the NSLS utilize a wide range of techniques and have one of the largest user groups with a single unifying theme at the NSLS, comprising nearly 30% of all registered users at the facility. The experiments have as their goal the identification of details of molecular chemistry and structure that explain the functions of biomolecules and cells. Macromolecular crystallography is used to provide detailed structural information, for example, about protein-DNA binding or protein-drug interactions. In cases where biomolecules cannot be crystallized, small-angle scattering can be used to follow structure changes. When detailed structure changes of protein active site metals are important to the function, EXAFS spectroscopy is commonly used to provide structure information. Microscopy techniques, like infrared and soft x-ray imaging, extend the range of biological investigations from the examination of chemical and structural information on biomolecules to the study of integrated biological systems, like cells.

Macromolecular Crystallography

A good example of a protein structure determination that relied on complementary features of two different beam lines, was that of the SecA translocation ATPase, by J. Hunt and J. Deisenhofer (Howard Hughes Medical Institute and the U. of Texas Southwestern Medical Center), and D. Oliver (Wesleyan U.). This work was carried out on beam lines X12B and X4A. SecA is a homologue of the family of membrane transport proteins known as ATP binding-cassette, or ABC, transporters, which couple the hydrolysis of ATP to the active transport of ligands across membranes. These proteins are of strong medical and pharmacological interest, and include, for example, the cystic fibrosis transmembrane conductance regulator (CFTR) and the P-glycoproteins which mediate the multidrug resistance phenotype observed in many tumor cells.

It is quite difficult to undertake high-resolution structural studies of integral membrane proteins, but insight into their basic structural organization can be gained by studying structural and functional homologues such as SecA, a soluble enzyme which functions in translocating secretory proteins through the bacterial periplasmic membrane. It is believed to function as a molecular ratchet in the protein translocation reaction, pulling segments of the secretory protein through the membrane in conjunction with ATP-driven membrane insertion cycles.

The high-resolution structure (to 2.9 Å) of the membrane-retracted state of SecA was determined from crystallography data collected on X12B. Data were collected on a native crystal and from various derivatives, for which the high beam line intensity and wavelength tunability (to effect measurements of anomalous differences in the diffraction patterns) allowed for rapid screening. A selenomethionyl derivative data set was measured on X4A, taking advantage of the strong anomalous scattering at the Se K absorption edge and the excellent energy resolution of that beamline. While the selenomethionyl derivative crystals didn't grow large enough to allow for their direct use in multiwavelength anomalous diffraction (MAD) phasing, this data set was still useful for pinpointing the methionine locations. The overall preliminary structural refinement points to the need to collect further data from SecA and its complexes with various physiological ligands at even higher resolution, yet a working model for rearrangements of its ATP-binding domains in the course of the transport cycle has already been formulated on the basis of the data collected.

A macromolecular crystallography program was begun on beam line X9B in 1996 by Albert Einstein College of Medicine. A group from this institution led by S. Almo, Z.-Y. Zhang, and D. Lawrence has spearheaded an effort to design potential therapeutic agents for and understand the structures of protein tyrosine phosphatases, whose roles in oncogenesis and signal transduction are of great significance. The structure of PTP1B (human protein tyrosine phosphatase 1B), complexed with several synthetic non-peptide substrates, has been solved to a resolution of 1.9 Å. Data were collected using Fuji imaging plates, which were read out via an off-line scanner. These results have given insight into phosphotyrosine binding sites, information that is crucial to the design of a new class of tight-binding inhibitors specific to the phosphatase. This is becoming of importance as the role of PTB1B in oncogenesis and non-insulin diabetes mellitus becomes clear.

The arrest of DNA replication in response to the detection of DNA damage is a fundamental mechanism by which the cell minimizes the potential transmission of lethal mutations. A primary mediator of this response is the protein p21WAF1/CIP1, an inhibitor of the cyclin dependent protein kinases that also binds to and blocks the action of DNA polymerase enzymes directly. An elevation of nuclear levels of the tumor suppressor protein p53 occurs upon detection of DNA damage. This thereby stimulates transcription of p21WAF1/CIP1 as part of a

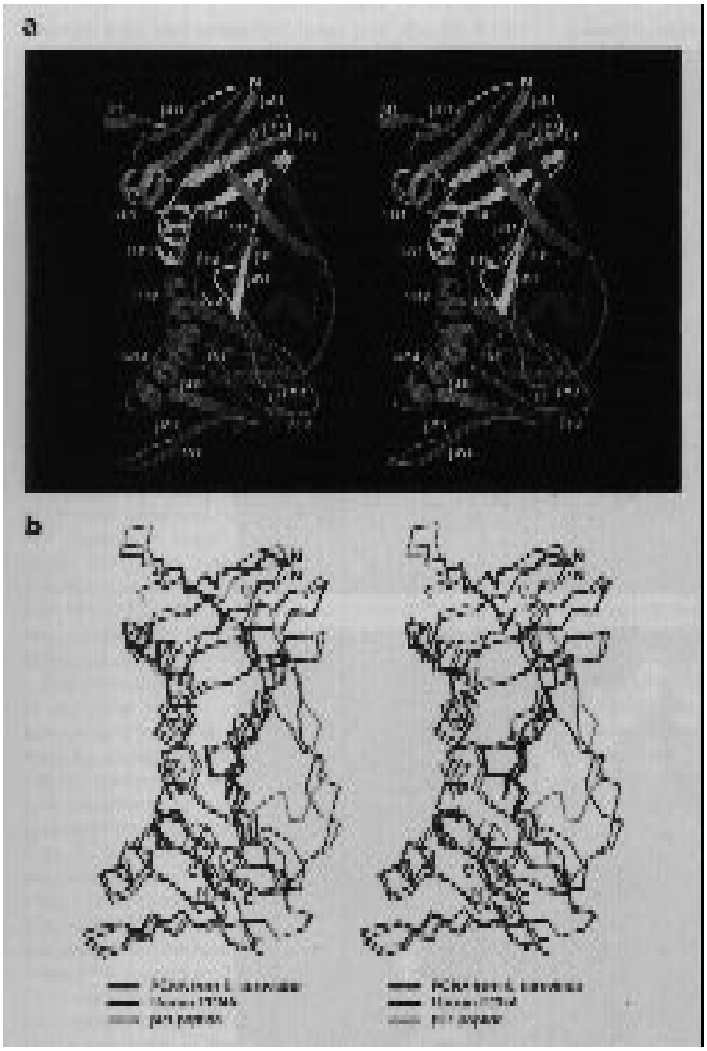

Figure 14: Ribbon diagram of the PCNA monomer with bound p21 peptide. (a) Stereo diagram of the three-dimensional structure of one monomer of the PCNA-p21 peptide complex, looking directly onto the face of the ring. The peptide (colored red) runs alongside the interdomain connecting loop (green). The N-terminal domain of PCNA is drawn in yellow and the C-terminal domain in plum, with five residues at the terminus shaded blue.
(b) Superimposition of the C^{α} trace of PCNA from *S. Cerevisiae* (red) onto that of human PCNA (black) with bound p21 peptide (green). The orientation is similar to that in (a). (X25)

p53 signalling pathway, via which the cessation of DNA replication is coupled to the stalling of cellular mitosis.

Using crystallography data measured at the wiggler beam line X25, a group led by J. Kuriyan (Howard Hughes Medical Institute and Rockefeller U.) determined the structure of the complex of the C-terminal region of p21WAF1/CIP1 with the human DNA polymerase delta processivity factor PCNA (proliferating cell nuclear antigen), to a resolution of 2.6 Å (work to be published in *Cell* by J. Gulbis, Z. Kelman, E. Gibbs, J. Hurwitz, M. O'Donnell, and J. Kuriyan). PCNA is a circular protein that encircles DNA and allows the polymerase to ride on it without dissociation during DNA replication, by forming a sliding clamp that tethers the polymerase to DNA during strand synthesis. The ability of p21WAF1/CIP1 to inhibit the action of PCNA may be due to its masking of PCNA elements that are required for the binding of components of the polymerase assembly. The derived structure (Figure 14) provides a view of a disabled PCNA molecule, which maintains a closed ring structure but is unable to support DNA replication. It also maps regions of the PCNA surface that might be important for polymerase attachment, and these are potential targets for the design of molecular analogs that would mimic the action of p21WAF1/CIP1.

Low Angle Scattering

Small angle scattering was used by K. Poole and K. Holmes (Max Planck Institute) and collaborators, on beam line X9B, to gain insight into structural differences between different muscle fiber complexes. Specifically, the motor protein myosin was isolated from both chicken skeletal and smooth muscles, and then introduced and bound to actin filaments in rabbit psoas muscle fibers. Small angle diffraction patterns were first measured from the two types of actomyosin complexes, and found to be different. Subsequent binding of the nucleotide ADP to each of these complexes resulted in little change to the diffraction pattern of the actomyosin complex derived from skeletal muscle myosin, but substantial change to the pattern of the complex derived from smooth muscle myosin (Figure 15, see next page), which became similar to the pattern associated with skeletal muscle myosin. These findings imply that at least some part of the power stroke associated with the motor function of these two kinds of muscle arises from different configurational changes of the actomyosin complex. While the data are still being analyzed, this already represents a novel finding and will be an intense subject of future study.

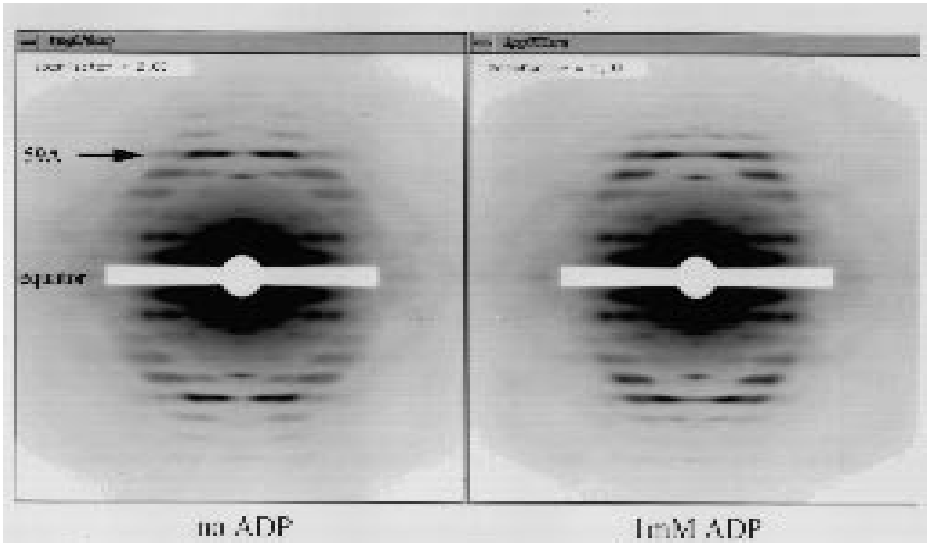

Figure 15: The effect of ADP on smooth-S1 decorated skeletal muscle action on low angle diffraction pattern. (X9B)

Crystal Growth for Macromolecular Crystallography

The growth of crystals that diffract well is the major rate limiting step in the collection and analysis of structural data from crystallography. The growth of such crystals, despite the improvements provided by mass screening procedures, is still an art. Thus it is important to try and quantify the results of a given growth procedure. One technique, used widely in materials science, is x-ray topography. Topography provides information specifically about crystalline perfection.

An experiment performed by V. Stojanoff (European Synchrotron Radiation Facility) and D.P. Siddons (National Synchrotron Light Source), E. Snell (National Aeroeronautical and Space Agency), and T. Boggon and J. Helliwell (U. of Manchester), on beamline X26C, addressed the study of crystalline perfection of various proteins grown in space (zero gravity conditions) and on earth (earth gravity conditions). Triple-axis diffractometry and x-ray topography were employed to characterize the samples. Using Si(111) monochromator and analyzer crystal reflections, the resolution in reciprocal space was sufficient to reveal fine structure in some of the Bragg peaks that would not have been resolvable using conventional double-axis diffractometry; employing triple-axis resolution, Bragg peaks were observed to be split in some instances. Fine structure in these peaks could be isolated and were further studied with x-ray topography, to provide insight into the spatial nature of crystallite domains responsible for the fine structure. From these studies, no definitive differences in the quality of the two classes of protein crystals (grown in zero gravity vs. in earth gravity) were revealed. These topography studies demonstrate a detailed method of examining crystal quality and may lead to a better evaluation of methods of crystal growth.

Micro-Spectroscopy Techniques

Synchrotron Radiation is well suited to spectroscopy on the μm scale due to the superior collimation and brightness compared to conventional sources. These advantages are illustrated in several biological applications, using infrared and x-ray radiation to interrogate a number of spectral transitions of interest. Thus, specific chemical information is derived associated with specific cellular structures.

Though the infrared absorption features of various organic molecules are well-known, very little work exists that relates specific infrared signatures with particular ultra-structural features in cells and tissues. Much of this is due to the small size scale frequently encountered. Several groups have begun investigations into biological tissues, and a few of the results from beamline U2B are described below.

One application of infrared microspectroscopy is for the identification and classification of various diseases in tissue samples. In a collaboration between the NRC (Canada), U. Manitoba, Kansas State U., and the U. Kansas Medical Center, Lin-P'ing Choo and coworkers studied microtomed sections from Alzheimer's diseased brain tissue. By following the shift of the amide I band from 1651 cm^{-1} to 1631 cm^{-1} (associated with b-amyloid), a map of diseased locations in a tissue region was obtained.

Developing non-destructive techniques is particularly important since alternative methods, such as chemical staining, can destroy the biochemical integrity of the tissue. In related work by the same collaboration, D.L. Wetzel (Kansas State U.) examined brain tissues exhibiting multiple sclerosis, and identified spectroscopic features directly associated with diseased regions.

Measurements on single living cells were conducted for the first time by N. Jamine, P. Dumas, and coworkers from DIEP-CEA, the Institute Curie and LURE (all in France) as well as the NSLS. A technique was developed whereby live cells (mouse hybridoma B) are dispersed onto BaF_2 substrates. The cells, which are about 20 μm across, remain alive for several hours. Also there is no evidence that the incident synchrotron infrared (~10 mW, or 100mW/mm^2) causes damage. Various cells were spectroscopically mapped using an effective aperture size of 3 μm. In this situation, diffraction limits the spatial resolution to a size scale ~10 μm. The IR spectra for the cells (Figure 16) show absorption features that can be attributed to particular chemical species. For example the absorption at 2920 cm^{-1} is due to the C-H stretch of aliphatic methylene groups associated mostly with lipids and proteins. As these lipids and proteins are found to be non-uniformly distributed within the cell, the chemical maps of the cell shown in Figure 15, and the relationship between the lipid distribution and cell division (mitosis) is one area of intense interest.

The soft x-ray microscope on beamline X1A is capable of imaging with chemical sensitivity by appropriately combining frames collected at photon energies which correspond to maxima and minima in absorption spectra. J. Boese, A. Osanna, C. Jacobsen, J. Kirz, E. Tall (SUNY @ Stony Brook) and X. Zhang (Harvard U.) are exploring the possibilities of protein specific imaging, ie mapping the concentrations of selected proteins in biological systems. As first steps, they have collected carbon K-edge near edge spectra of pairs of amino acids and compared them to the spectra of the corresponding dipeptide (the two amino acids bound via a peptide bond). As shown in Figure 17 (see next page), the researchers found in the case of glycine and tyrosine that the spectrum of the dipeptide is very close to a simple sum of the individual spectra. The formation of the bond had only a small effect, a ~0.3 eV shift in the C 1*s*-π* peak at 289 eV. If this result holds true for arbitrary combinations of amino acids, the absorption spectra of simple proteins can be predicted. (However, the inverse problem is made more difficult: given a spectrum, there is no information regarding the amino acid order or whether there are multiple molecules.)

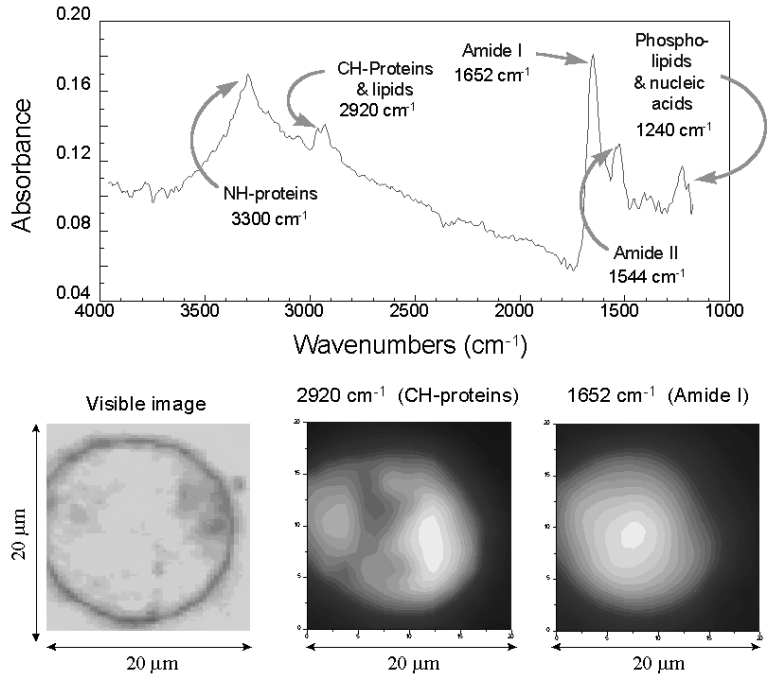

Figure 16: Infrared microspectroscopy study of a live cell. Top: A typical absorption spectrum for the cell, with various absorption modes identified. Bottom: visible and IR images, showing distribution of cellular substances. (U2B)

X-Ray Absorption Spectroscopy

Zinc is ubiquitous in biological systems, appearing in countless metalloenzymes. It is found, for example, in the active sites of many proteases, metalloproteins which cut other proteins in half at sites with specific amino acid sequences. One of the most interesting fundamental biological questions currently being addressed with micro-x-ray absorption spectroscopy concerns the egg. As an essentially closed system it must be preloaded with the full complement of metals required for complete development. In work on beamline X19A, K. Pariso, C. van Huis, R. Denver, and J. Penner-Hahn (U. of Michigan) have been studying the structural evolution of

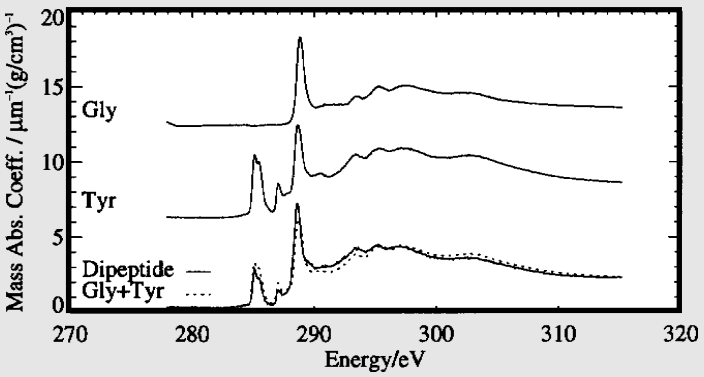

Figure 17: The x-ray absorption spectra of glycine, tyrosine, and a Gly-Tyr dipeptide (solid lines) are shown together with a weighted sum of the two monomer spectra (dashed line). (X1A)

the 1 mM zinc found in zebrafish and African clawed toad (*Xenopus*) eggs as a function of time after fertilization. Due to the mm dimensions and high zinc concentration of these eggs, they offer a strong zinc signal on beamline X19A. Transcription factors, called zinc fingers, play important roles in early development. The spectra in Figure 18 show the large changes in zinc structure that occur during development from single cell to late blastula phase. This suggests substantial synthesis of new classes of zinc proteins during these developmental phases.

Figure 18 shows Zn k-edge XANES difference spectra relative to an unfertilized (nondeveloping) egg at various stages in the embryo development. Changes are clearly evident even in the first few cell divisions. The researchers note that the changes indicate the formation of multiple zinc sites in a complex process. Planned extensions to this work include two and three dimensional imaging of metal concentrations.

The use of EXAFS and XANES to examine the metal center structure in metalloproteins has been one of the most popular applications of synchrotron technology in biology since the initial phases of synchrotron development. The ability to derive metal-ligand bond length information on dilute and chemically poised samples of metalloproteins is extremely valuable in understanding mechanisms of protein function. Biological molecules are, of course, often large and difficult to study with conventional spectroscopies. The element specificity of XAS techniques make them useful for ignoring the background of thousands of amino acid residues to focus on the local structure around metals or other heavy elements. They complement 2d NMR studies and protein crystallography by determining oxidation states and precise bond lengths, metal properties that are essential for fully understanding active site structure function.

For example, in recent work on X9B, H. Anni (Thomas Jefferson Medical College), J. Vanderkooi (U. of Pennsylvania), M.R. Chance, and E. Scheuring (Albert Einstein College of Medicine) studied the structure of zinc II substituted cyctochrome c. NMR studies had proposed a six coordinate zinc site with five nitrogens and one sulfur as ligating atoms. This structure is highly unusual, there are no previously known six coordinate zinc sites in biological molecules in solution. However, XAS studies followed by refinement against theoretical models indeed confirmed the Zn site as six coordinate, with bond lengths resolved as Zn-N (porphyrin core) = 2.05 Å, Zn-N (histidine) = 2.10-2.20 Å, and Zn-S = 2.34 Å. In denatured protein, the zinc was found to have lost the sulfur coordination. The researchers conclude that the unique zinc environment must be imposed by the protein structure.

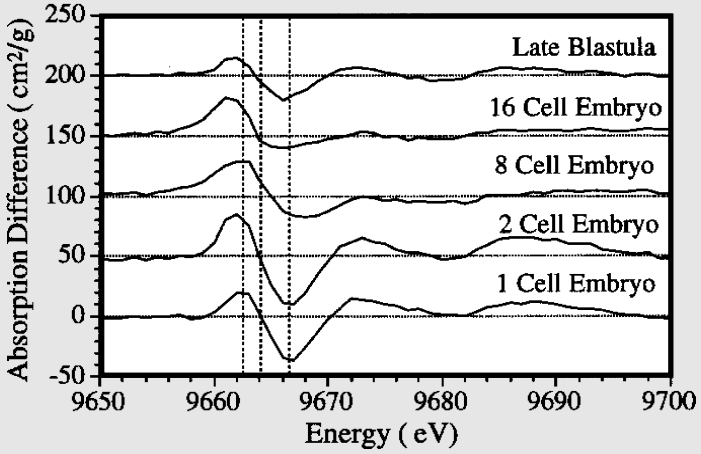

Figure 18: Time-dependent Zn XANES spectra of *Xenopus* eggs following fertilization. Spectra shown are difference spectra relative to an unfertilized control sample. Vertical dashed lines at 9662.5 eV, 9664.1 eV, and 9666.6 eV mark the critical points for the 1 cell difference spectrum, illustrating the change in spectra with time. (X19A)

The study of metalloenzyme chemistry by L. Que and co-workers (U. of Minnesota) on beamline X9B has been particularly focused on non-heme iron proteins and the activation of molecular oxygen to carry out oxygen insertion chemistry. For methane monooxygenase, EXAFS analysis has shown two Fe-Fe distances of about 3 Å and 3.4 Å which may reflect two populations of the enzyme with varying diiron (III) core structures.

L. Powers and co-workers (U. of Utah), using beamline X9B, have continued their examination of heme iron containing enzymes, called peroxidases, which, unlike the diiron proteins, use hydrogen peroxide to oxidize iron to the unusual Fe(IV) valence. These hi-valent iron species and associated protein radicals then are used to oxidize various substrates depending on the peroxidase. Site directed mutagenesis studies that varied the basicity of the iron coordinating ligands were correlated with specific iron-nitrogen bond length changes. As the basicity of the histidine axial ligand was increased by changing the hydrogen bonding to the remote nitrogen, the distance from iron to the directly coordinated nitrogen of the histidine axial ligand decreased by 0.15 Å. This definitively demonstrated that changes in hydrogen bonding 3-4 Å from the metal site can control structure and functionality of the iron site through coupling of the iron to the histidine pi electronic system.

M. Chance and co-workers (Albert Einstein College of Medicine) also carried out studies of heme metalloproteins on beamline X9B, in this case the oxygen transport protein myoglobin was examined. Synchrotron crystallography experiments by I. Schlichting (Max Planck Institute), J. Berendzen (Los Alamos National Laboratory) and co-workers carried out on beamline X12C had identified a "docking" site for the ligand, essentially identifying a way station for the ligand on its way to its binding site coordinated to the heme iron. These results had been challenged by other crystallography groups. EXAFS experiments were carried out by the Chance group examining the same intermediate. In addition, a new global mapping procedure, where crystallographic coordinates are refined to EXAFS data using the *ab initio* EXAFS code FEFF, (discussed also below) was used to show that the Berendzen structure is essentially correct.

The global mapping procedure was also used to examine metalloprotein structure in cobalamin enzymes by Chance and co-workers (Albert Einstein College of Medicine) in collaboration with scientists from U. of Michigan and U. of Nebraska, using beamline X9B. Cobalamin co-factors are cobalt containing prosthetic groups containing cobalt-carbon bonds, and are the only known organometallic species in the biological realm. Some similarities exist with the hemeproteins, in that an axial histidine ligand coordinates the metal perpendicular to the planar organic cofactor. The enzymes carry out unusual carbon-carbon bond re-arrangements and methylation reactions critical for cell metabolism. Mutant forms of the enzyme, methionine synthase, were examined, where the axial histidine is replaced with various amino acids. The changes in electronic structure at the cobalt ion, and the role of the histidine ligand in controlling enzyme activity were better understood as a result. The global mapping technique is illustrated in Figure 19, where particular minima based on the FEFF simulations can be directly compared to each other in an evenhanded manner.

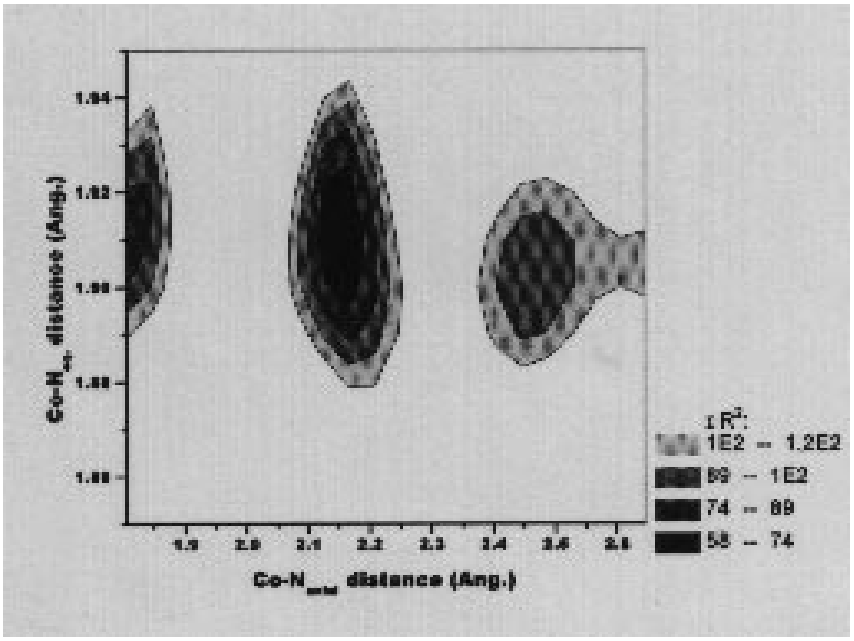

Figure 19: A contour plot of the goodness-of-fit versus FEFF 6.01 simulation geometry for the Adenosylcobalamin cofactor reconstituted into methylmalonyl CoA-mutase. (X9B)